Journal of Visualized Experiments

Pathological Analysis of Lung Metastasis Following Lateral Tail-Vein Injection of Tumor Cells

--Manuscript Draft--

Article Type:	Invited Methods Collection - JoVE Produced Video
Manuscript Number:	JoVE61270R2
Full Title:	Pathological Analysis of Lung Metastasis Following Lateral Tail-Vein Injection of Tumor Cells
Keywords:	tail-vein injection; breast cancer; lung metastasis; H&E-stained sections; quantitative digital pathology; image analysis
Corresponding Author:	Steven T Sizemore, Ph.D. Ohio State University Columbus, Ohio UNITED STATES
Corresponding Author's Institution:	Ohio State University
Corresponding Author E-Mail:	steven.sizemore@osumc.edu
Order of Authors:	Katie A Thies
	Sue E Knoblaugh
	Steven T Sizemore, Ph.D.
Additional Information:	
Question	**Response**
Please indicate whether this article will be Standard Access or Open Access.	Standard Access (US$2,400)
Please indicate the **city, state/province, and country** where this article will be **filmed**. Please do not use abbreviations.	Columbus, Ohio, USA

TITLE:

Pathological Analysis of Lung Metastasis Following Lateral Tail-Vein Injection of Tumor Cells

AUTHORS AND AFFILIATIONS:

Katie A. Thies[1], Sue E. Knoblaugh[2], Steven T. Sizemore[1]

[1]Department of Radiation Oncology, Arthur G. James Comprehensive Cancer Center and Richard L. Solove Research Institute, The Ohio State University Medical Center, Columbus, Ohio

[2]Department of Veterinary Biosciences, Comparative Pathology and Mouse Phenotyping Shared Resource, The Ohio State University, Columbus, Ohio

Email addresses of co-authors:

Katie A. Thies (Katie.Thies@osumc.edu)

Sue E. Knoblaugh (Knoblaugh.1@osu.edu)

Corresponding author:

Steven T. Sizemore (Steven.Sizemore@osumc.edu)

KEYWORDS:

tail-vein injection, breast cancer, lung metastasis, H&E-stained sections, quantitative digital pathology, image analysis

SUMMARY:

Intravenous injection of cancer cells is often used in metastasis research, but the metastatic tumor burden can be difficult to analyze. Herein, we demonstrate a tail-vein injection model of metastasis and include a novel approach to analyze the resulting metastatic lung tumor burden.

ABSTRACT:

Metastasis, the primary cause of morbidity and mortality for most cancer patients, can be challenging to model preclinically in mice. Few spontaneous metastasis models are available. Thus, the experimental metastasis model involving tail-vein injection of suitable cell lines is a mainstay of metastasis research. When cancer cells are injected into the lateral tail-vein, the lung is their preferred site of colonization. A potential limitation of this technique is the accurate quantification of the metastatic lung tumor burden. While some investigators count macrometastases of a pre-defined size and/or include micrometastases following sectioning of tissue, others determine the area of metastatic lesions relative to normal tissue area. Both of these quantification methods can be exceedingly difficult when the metastatic burden is high. Herein, we demonstrate an intravenous injection model of lung metastasis followed by an advanced method for quantifying metastatic tumor burden using image analysis software. This process allows for investigation of multiple end-point parameters, including average metastasis size, total number of metastases, and total metastasis area, to provide a comprehensive analysis. Furthermore, this method has been reviewed by a veterinary pathologist board-certified by the American College of Veterinary Pathologists (SEK) to ensure accuracy.

INTRODUCTION:

Despite being a highly complex and inefficient process[1], metastasis is a significant contributor to the morbidity and mortality of cancer patients[2]. In fact, most cancer-related deaths are attributed to metastatic spread of disease[3,4]. In order for tumor cells to successfully metastasize, they must detach from the primary site, invade through adjoining stroma, intravasate into blood circulation or lymphatics, travel to the capillary bed of a secondary site, extravasate into the secondary tissue, and proliferate or grow to form metastatic lesions[5]. The use of mouse models has been critical to furthering the understanding of the molecular mechanisms responsible for metastatic seeding and growth[6,7]. Herein, we focus on breast cancer metastasis, for which both genetically modified mouse models as well as methods of transplantation are often used – each with their own set of advantages and limitations.

Genetically engineered mammary tumor models make use of mammary gland specific promoters, including *MMTV-LTR* and *WAP* (Whey Acidic Protein), to drive expression of transgenes in the mammary epithelium[8]. Oncogenes including polyoma middle T antigen (*PyMT*), *ErbB2/Neu*, *c-Myc*, *Wnt-1*, and simian virus 40 (*SV40*) have been expressed in this manner[9-13], and while these genetic models are useful for studying primary tumor initiation and progression, few readily metastasize to distant organs. Furthermore, these genetic mouse models are often more time and cost prohibitive than spontaneous or experimental metastasis models. Given the limitation of most genetically engineered mammary tumor models to study metastasis, transplantation techniques have become an attractive model to study this complex process. This includes orthotopic, tail-vein, intracardiac, and intracranial injection of suitable cell lines.

Although several breast cancer cell lines readily metastasize following orthotopic injection into the mammary fat pad[14,15], the consistency and reproducibility of metastatic tumor burden can be a challenge, and the duration of such studies can be on the order of several months. For evaluating lung metastasis, in particular, intravenous injection into the tail-vein is often a more reproducible and time-effective method with metastatic spread typically occurring within the span of a few weeks. However, since the intravenous injection models bypasses initial steps of the metastatic cascade, care must be taken in interpreting the results of these studies. In this demonstration, we show tail-vein injection of mammary tumor cells along with an accurate and comprehensive method of analysis.

Even though the research community has made significant progress in understanding the complex process of breast cancer metastasis, it is estimated that over 150,000 women currently have metastatic breast cancer[16]. Of those with stage IV breast cancer, >36% of patients have lung metastasis[17]; however, the site-specific pattern and incidence of metastases can vary based on molecular subtype[18-21]. Patients with breast cancer lung metastases have a median survival of only 21 months highlighting the need to identify effective treatment and novel biomarkers for this disease[17]. The use of experimental metastasis models, including the intravenous injection of tumor cells, will continue to advance our knowledge of this important clinical challenge. When combined with digital imaging pathology and the method of metastatic lung tumor burden analysis described within this protocol, tail-vein injections are a valuable tool for breast cancer metastasis research.

PROTOCOL:

Animal use followed University Laboratory Animal Resources (ULAR) regulations under the OSU Institutional Animal Care and Use Committee (IACUC)–approved protocol 2007A0120-R4 (PI: Dr. Gina Sizemore).

1. Tail-vein injection of breast cancer cells

1.1. Preparation of cells and syringe for injection

1.1.1. Plate an appropriate number of cells based on the number of mice and cell concentration to be used.

NOTE: The number of cells injected and time to the development of metastases will depend on the cell line used and will need to be optimized. In this demonstration, 1 x 10^6 MDA-MB-231 cells are injected intravenously into nod scid γ (NSG) mice, and macroscopic lung lesions are observed no later than 24 days post-injection. For the MVT1 murine mammary tumor cell line[17], 3 x 10^6 cells are injected into immune-competent FVB/N mice with numerous lung metastases observed by 14 days[22,23].

1.1.2. Aspirate media and rinse cell plates with 1x PBS. Trypsinize cells in minimal volume, add appropriate volume of media, and count cells using a hematocytometer or another preferred method. Trypan blue (0.4%) or other live/dead cell dyes can be used to determine viable cell counts.

1.1.3. Pellet cells by spinning at 180 x *g* for 5 min.

1.1.4. Resuspend appropriate number of cells in sterile 1x PBS such that a volume of 100 µL is injected per mouse. Keep cell suspension on ice to maintain viability.

1.1.5. Prior to injection, thoroughly resuspend cells with a 200 µL or 1 mL pipette to avoid clumping. Draw up 100 µL in a 28 G insulin syringe (see **Table of Materials**).

1.1.6. Eliminate any air bubbles by keeping the syringe vertical, tapping on the syringe and slowly adjusting the plunger. Injection of air bubbles into the vein is likely to cause an air/gas embolism that can be fatal.

1.2. Lateral tail-vein injection

NOTE: For experimental breast cancer metastasis assays, injections are performed on > 6 weeks old female mice.

1.2.1. Handle the mouse by the tail and slide animal into a slotted tube/restraint device of an appropriate size (see the **Table of Materials** for restraint device used).

1.2.2. Insert the plug portion of the restraint device and position the mouse on its side such that its lateral tail vein is easy to view. The mouse has a ventral artery in line with the genitalia, a dorsal vein, and two lateral caudal veins.

1.2.3. Clean the surface of the mouse's tail with an aseptic wipe. Grasp the tail between index finger and thumb with non-dominant hand and apply slight tension.

1.2.4. Beginning at the distal portion of the tail, insert the needle parallel to the vein with the bevel end up.

1.2.5. If allowed, *carefully* recap the needle and bend to a 20-30° angle. A single-handed approach or needle recapping device is highly recommended.

NOTE: It is not necessary to aspirate as this may cause the vein to collapse. However, a small flash of blood may be seen when first placed. The needle will advance smoothly into the vein with proper placement.

1.2.6. Slowly dispense the complete volume into the vein. There should not be resistance when the plunger is pushed.

1.2.7. If any resistance is felt, promptly remove the syringe needle. If needed, re-insert the needle (ideally no more than 3 attempts) moving toward the proximal end of the tail or opposing lateral vein.

1.2.8. A small volume of blood will likely be displaced after injection. Apply gentle pressure with sterile gauze and wipe with aseptic wipe.

1.2.9. Promptly dispose of syringe in appropriate sharps container.

1.2.10. Return the mouse to a clean, ventilated cage and monitor for signs of distress.

1.2.11. Monitor mice for signs of metastasis formation and distress (ideally, 3x weekly). The time to development of metastasis will depend on cell line and mouse strain.

1.2.12. If using an in vivo live animal imaging device, image mice immediately after tail-vein injection to confirm successful injection of cells and obtain time "zero" data (specific details on in vivo bioluminescence imaging are not included herein, but are described by Yang et al.[24]).

2. Lung tissue fixation and analysis of metastatic lung tumor burden

2.1. Lung tissue inflation to maintain the structural format of the lungs for histopathology

2.1.1. After approved euthanasia procedures are followed, secure the mouse carcass to a dissecting board with pins. Either spray or apply 70% ethanol to keep the mouse's fur out of the way during dissection.

2.1.2. Open the thorax with a midline incision, extend the incision cranially/caudally through the peritoneum, and cut away the diaphragm by grasping the xyphoid process.

2.1.3. Using a separate set of scissors to not dull the blades, cut the ribs along each side of the sternum and carefully remove rib cage leaving room for the lungs to expand.

2.1.4. Isolate the trachea by removing submandibular salivary glands and infrahyoid musculature. Placing pins on either side of the trachea can prevent unwanted movement during needle insertion.

2.1.5. Fill a 26 G syringe with 2-3 mL of 10% neutral buffered formalin and insert into the trachea.

2.1.6. Slowly inject formalin and watch for the lungs to expand (usually requires ~1.5 mL of formalin).

2.1.7. Once formalin begins leaking out of the lungs (avoid over inflation), pinch off the trachea with a pair of forceps, remove syringe needle and detach the entire respiratory apparatus. Place lungs, heart, etc. directly into formalin as additional trimming of tissue can be done post-fixation.

2.1.8. Complete processing, embedding, sectioning of tissue, and hematoxylin and eosin (H&E) staining using standard methods.

2.2. Analysis of metastatic lung tumor burden

2.2.1. Scan H&E-stained lung sections on a high-resolution, slide scanner at 40x magnification (**Figure 3**).

2.2.2. Import images into image analysis software (e.g., Visiopharm Image Analysis) for quantification of lung metastases.

NOTE: We recommend that new users either obtain onsite or online training to use the image analysis software. Numerous webinars are also available through the commercial webpage.

2.2.3. Select the Visiopharm 10118 H&E Lung Metastasis App from the software's app library.

NOTE: The purpose of this app is to label and quantify lung metastasis on H&E-stained slides. As part of the 10118 H&E Lung Metastasis App, the first image processing step segments the lung tissue with the Tissue Detection App. The second image processing step uses the Metastasis Detect App which identifies the metastases inside the lung tissue. Metastases are identified via

shape together with regions that are either too misshaped, too red or too sparse for being identified as metastases.

2.2.4. Adjust the parameters defining shape and sparseness to best fit representative images. Segmented areas of tumor metastases and normal lung tissue can be displayed using different color labels for each tissue type.

NOTE: In the event that the app cannot accurately separate metastases from normal lung tissue, a custom app using the Visiopharm Decision Forest program may need to be written as was done for the experiments (see **Figures 2 and 3**). Details for writing a custom algorithm follow below. Otherwise, proceed to step 2.2.9.

2.2.5. Open the Decision Forest program, which works by training multiple **Classes** [i.e., lung tissue (non-neoplastic), metastases, red blood cells, epithelium, and/or white space] on a desired image. In **Figure 2**, tumor metastases are blue, normal tissue is green, and bronchiolar epithelium is yellow. Also, red blood cells are in red and air spaces in pink.

2.2.6. Follow the prompted series of yes or no questions to appropriately train each **Class** for an image. The accuracy of the algorithm will determine the number of yes/no questions. For the analysis, the custom algorithm/App was written with accuracy set to 50 (range 0-100).

2.2.7. Adjust **Features** for each class by applying filters to sharpen, blur, sort by shape, etc. to enhance the accuracy of the algorithm/App. Visiopharm views each **Class** through one or multiple lenses known as **Features**. **Features** change how the **Class** sees the image to bring out certain colors or intensities.

NOTE: For the custom algorithm, metastases measuring 8500 μm^2 and above are labeled and measured as metastases. This accounts for size variance and metastases too small to detect. Small misshaped areas and small metastatic areas under 8500 μm^2 were included in the normal tissue quantification.

2.2.8. Save the modified settings from either the app or custom algorithm and then, apply the algorithm/app to an entire set or series of H&E-stained tissues.

2.2.9. Finally, export all output variables, which includes those listed in **Table 1**. Area in microns squared (μm^2) can be quantified for each tissue type and percentages are derived from specimen total net tissue area (i.e., total tissue minus air space).

2.2.10. When creating a custom algorithm, review tissue markups in consultation with a veterinary pathologist board-certified by the American College of Veterinary Pathologists to ensure accurate measurements and differentiate between tissue types.

REPRESENTATIVE RESULTS:

If using unlabeled cells for tail-vein injection, it may be difficult to confirm lung colonization until (1) the time of necropsy if macrometastases can be observed or (2) following histological analysis if microscopic metastases exist. With extensive metastatic lung tumor burden, mice will have labored breathing. As with any tumor study, mice should be carefully monitored throughout the study duration. The use of labeled cells is an easy way to confirm successful tail-vein injection; hence the use of luciferase-tagged MDA-MB-231 cells in the demonstration. However, in vivo imaging is not always possible or necessary depending on the experimental design and other factors. **Figure 1A** shows bioluminescence signal in the thoracic space less than 2 hours after tail-vein injection of luciferase-tagged MDA-MB-231 cells as confirmation of accurate injection. For this experiment, photon counts in the thoracic region increase over time and a strong bioluminescence signal is present at day 24 post-injection (**Figure 1B and C**; note the change in scale bar). At the time of necropsy, many macroscopic lung lesions were observed in these mice (**Figure 1D**).

After proper tissue processing and staining, H&E-stained lung sections can be scanned or imaged. Metastatic lung tumor burden quantification can be effectively achieved using image analysis software and a custom algorithm. Using this algorithm, whole lung tissue is segmented by different tissue features (**Figure 2A and B**). By segmenting the lung tissue in this manner, the software can quantify the various parameters listed in **Table 1**. This analysis has been performed on lung tissue from mice injected with MDA-MB-231 cells followed by treatment with a drug designed to block metastatic colonization or a vehicle control (DMSO). The raw data from this analysis are shown in **Table 2**. Furthermore, **Figure 3A** shows representative H&E images of MDA-MB-231 lung metastases from either DMSO or drug-treated mice. While a difference in metastatic tumor burden between these treatment groups may have easily been overlooked as the total number of lung nodules is no different, a comprehensive analysis of all parameters indicates a significant difference in the percent net lung metastasis area (**Figure 3B,C**). This underscores the need for a comprehensive and thorough approach to analyze metastatic lung tumor burden such as the method described herein.

For the data presented in **Figure 3**, all statistical analyses were conducted using GraphPad Prism 7. Data were considered normally distributed upon passing any of the following standard normality tests: D'Agostino-Pearson omnibus, Shapiro-Wilk, and Kolmogorov-Smirnov. Comparison between the vehicle and drug-treated groups (**Figure 3**) was done by homeoscedastic or heteroscedastic unpaired two-tailed Student's t-test as appropriate. Statistical significance was established at $P \leq 0.05$.

FIGURE AND TABLE LEGENDS:

Figure 1: In vivo bioluminescence confirmation of successful tail-vein injection. (**A**) Representative bioluminescence signal in mice 1 hour after tail-vein injection of luciferase-tagged MDA-MB-231 cells. (**B**) Representative bioluminescence signal in the same set of mice as (A) 24 days after tail-vein injection of luciferase-tagged MDA-MB-231 cells. [Note the change in scale bar between (A) and (B)]. (**C**) Quantification of photon counts over time in MDA-MB-231 tail-vein injected mice. Error bars represent mean ± SEM. (n = 8 mice) (**D**) Representative non-tumor

bearing lung tissue (right) and MDA-MB-231 macrometastases in the lungs (left) at time of necropsy. Scale bars = 50 mm.

Figure 2: Tissue segmentation using Visiopharm software. (**A**) Representative snips of unsegmented and segmented tissue mark-ups using the customized software algorithm. (**B**) Legend for all tissue categories segmented using software.

Figure 3: Representative metastatic lung tumor burden analysis of H&E-stained tissues. (**A**) Representative H&E staining of lung tissue from uninjected mice and control (DMSO) and drug-treated mice following tail-vein injection of MDA-MB-231 cells. Representative tumor metastases are indicated with arrows. Scale bars = 500 µm for 4x magnification and 200 µm for 10x magnification. (**B**) Graph of percent net lung metastasis area of control and drug-treated mice. Error bars represent mean ± SD. (*) $P = 0.022$ by Student's t-test. (**C**) Table summarizing the metastatic lung tumor burden analysis (n = 9 DMSO; n = 9 drug-treated). After checking for normal distribution of data, all *P*-values in the table were determined by unpaired, two-tailed Student's t-test.

Table 1: Parameters measured with software. List of parameters along with a description of each measurement that is computed using the custom algorithm.

Table 2: Representative table of results. Table of results for each parameter of the algorithm from a cohort of mice tail-vein injected with MDA-MB-231 cells.

DISCUSSION:

As researchers continue to use intravenous injection of tumor cells as an experimental model for metastasis, standard practices to analyze the resulting metastatic tumor burden are lacking. In some cases, significant differences in metastatic tumor burden upon manipulation of particular cell lines and/or use of chemical compounds can be observed macroscopically. However, in other instances, subtle differences in metastatic seeding and growth may be overlooked or misinterpreted without thorough pathological analysis. This study advances previously published tail-vein injection protocols by including a comprehensive method of metastatic lung tumor burden analysis. Importantly, this method of digital pathology analysis can also be applied to the quantification of lung metastatic tumor burden following orthotopic injection of tumor cells which are capable of spontaneous metastasis as well as other experimental metastasis models (i.e. intracardiac, etc.). The use of digital imaging and software algorithm development by veterinary pathologists ensures the reproducibility, accuracy, and thoroughness of this approach to analyze metastatic lung tumor burden[25].

Thoughtful decision of cell lines, cell concentration, and endpoints based on either previously published studies or careful experimental optimization is absolutely necessary. Given that metastatic seeding and colonization are highly dependent on interactions with various immune cell populations[26,27], the use of immune-competent mice is ideal, albeit not always feasible. For the same reason, the interpretation of experimental metastasis studies using athymic or NSG mice, which lack key immune cell components, should be taken with caution. There are several

mouse mammary tumor cell lines, including the MVT1 cells used in this study, that have been derived from FVB/N mouse strain[22,28,29]. Other syngeneic models exist as well. In regard to cell concentration, injection of a large number of cells may greatly accelerate and enhance metastatic lung tumor burden. However, if the lungs are overwhelmed, it may be difficult to distinguish individual metastatic foci and emboli are more likely to occur. Also, the tail-vein injection procedure requires ample practice and training before safely and/or routinely performing injections. Many institutions will offer technical training and may provide mice for practice purposes. Proper placement of the needle and a smooth injection should indicate success; however, for training/practice purposes, Evan's Blue dye can be used to help determine successful injection (1% in sterile PBS). The extremities of the mouse will turn blue shortly after injection, but the animal should be euthanized afterwards.

Additionally, the importance of standard necropsy and tissue sampling techniques to control and prevent slide artifacts that may impair slide scanning and analysis by the image analysis software cannot be stressed enough. Inflation of the lungs at time of necropsy is a critical step in maintaining tissue integrity and improves subsequent H&E staining as well as final analysis. For consistency with resolution and reproducibility, it is recommended that all slides in a study set are scanned with the same objective. In this study, all slides were scanned at 40x to ensure accuracy of algorithm settings and proper identification of tumor metastases when applied to analyzed fields. For each slide, the same lung lobes were consistently scanned and analyzed for each mouse. It is also strongly recommended that a pathologist review tissue markups for accuracy of the applied algorithm and that the same algorithm is applied to every slide in a study.

The presented protocol can be modified according to experimental design, user preferences, and desired outcome measurements. One such modification includes the use of an anesthesia induction chamber rather than conventional restrainer device for a conscious animal. In terms of animal health and wellness, neither approach is superior to the other and each has its own set of advantages as well as limitations[30]. Also, for black or brown mice, a light source or heating device may be needed in order to visualize the tail veins. Infrared lamps or a warm water bath can be used to dilate the veins. However, temperature should be carefully monitored. Furthermore, there are illuminated restraint devices available as well as other commercial versions of rodent restraint devices. Some investigators prefer Luer-Lok syringes for injections. We find it more difficult to eliminate air bubbles with Luer-Lok syringes, but it is a matter of preference. The viability of cells is an important consideration for the tail-vein injection procedure, and therefore, accurate cell counts as well as maintaining cells on ice prior to injection are necessary steps. If comparing lung seeding and colonization of manipulated cell lines, it is critical to determine any differences in cell size and viability prior to injection as these may complicate the interpretation of results. Cell death and/or damage may occur when using a narrow gauge needle; however, it is not recommended that a needle larger than 25 G be used as it may cause pain and discomfort to the animal.

As a way to validate that lung lesions are formed by injected tumor cells, immunostaining can be done on tissue sections. If using human cell lines, human-specific antibodies can be used to discern metastatic lesions. Alternatively, if using tagged cell lines (e.g., GFP), corresponding

antibodies can be used. Also, many breast cancer cell lines are positive for epithelial markers (i.e., cytokeratins, E-cadherin, and EpCAM), but prior knowledge of expression is essential. However, the lung epithelium lining the airways will also be positive for these markers and thus, structure must also be considered. There may be cases in which primary lung tumor development must be ruled out. For this, immunohistochemical staining for TTF1 (transcription termination factor 1) as a marker for primary lung adenocarcinoma can be used but tissues should also be evaluated by a certified pathologist.

Herein, a custom algorithm was written using a Decision Forest classification algorithm because the established lung metastasis algorithm could not be fine-tuned for accurate detection of metastases that varied in size. This customized algorithm enables complex measurements, allows for accurate segmentation of metastases by size, and supports a size cutoff so that small misshaped areas and normal structures are not misinterpreted and can therefore be included in the final data set. We anticipate that this algorithm will be applicable to most in vivo lung metastasis studies, but users may need to adjust settings within the software to fit their individual study needs. However, this algorithm serves as a platform for investigators wishing to analyze lung metastatic burden in a similar manner. There are many different options for image analysis platforms whereby access or availability, cost and training, as well as experience level may dictate the best platform to utilize[36]. The range of options include free platforms such as QuPath and more expensive, but sophisticated platforms, such as Visiopharm. It is advised that one consults with an image analysis pathology core and pathologist when deciding which platform may be available and best utilized for a particular research project.

Spontaneous mouse mammary tumor models (e.g., *MMTV-PyMT*) or orthotopic mammary fat pad injection methods represent the most physiologically relevant model for studying lung metastasis. A serious drawback to the tail-vein injection model is that it does not recapitulate the full metastatic cascade and is therefore limited to the study of tumor cell extravasation and secondary organ colonization. However, this experimental metastasis model is relevant for breast cancer research as lung metastases formed following tail-vein injection have genomic profiles similar to metastatic lesions that develop after orthotopic implantation of the same cells[31]. In order to establish a lung metastasis model, a large number of cells are often injected intravenously which may not accurately represent the process of metastasis as it pertains to seeding, immune reaction, and dormancy. Also, based on the circulatory pathway, pulmonary metastases are most common with tail-vein injection[32]. With most breast cancer cell lines, published reports indicate a relatively low incidence of bone, liver, or brain metastases following tail-vein injection[7]. Alternative experimental metastasis methods such as intracardiac, intratibial, portal vein and intracarotid injections are more appropriate for examining metastases to other sites[33-37]. Again, spontaneous mammary tumor models or orthotopic fat pad injection methods that recapitulate all steps of the metastatic cascade are preferred. Issues with consistent metastatic tumor burden, duration of study, and numbers of animals required for such studies are a downside. However, the method of digital pathology analysis presented here can be applied to lung metastases formed through any spontaneous or experimental metastasis model.

The method of analysis also yields certain limitations such as subjectivity in algorithm creation.

Even though whole slide imaging allows for digital analysis on an entire tissue section and on all lung lobes of a single mouse, it is limited to a two-dimensional analysis of a 3D tissue. Stereology is becoming a common practice that obtains 3D information for image analysis and can account for factors such as tissue shrinkage that occurs during tissue processing[38]. Stereology, however, has its own limitations such as tissue, resource, and time constraints.

Given the number of cancer patients affected by metastatic spread of their disease, the tail-vein injection method to study metastasis will continue to be a useful tool in terms of understanding the complicated biology of metastatic spread and in determining the pre-clinical efficacy of novel therapeutics. In vivo mouse models of metastasis, particularly those using immune-competent animals, are becoming even more important for cancer research given the widespread interest in immunotherapy[29]. Also, experimental metastasis models are critical in terms of investigating metastasis suppressor genes (i.e., those that suppress the metastatic potential of cancer cells without affecting primary tumor growth), and therefore, continue to be a valuable research tool.

Digital imaging and slide analysis have rapidly become a mainstay in diagnostic and experimental mouse modeling[39]. Using the type of approach described herein to analyze lung metastatic tumor burden will allow for high throughput analyses in a more comprehensive and accurate manner. Furthermore, digital imaging pathology provides an avenue for more collaborative research projects involving pathologists that specialize in areas such as mouse models of breast cancer metastasis. As multiplex tissue imaging methods and 3D imaging technologies (as mentioned above) continue to be developed, digital imaging pathology, sophisticated software programs for image analysis, and the expertise of pathologists will certainly be necessary for advancing metastasis research.

ACKNOWLEDGMENTS:

Representative data was funded through the National Cancer Institute (K22CA218549 to S.T.S). In addition to their assistance in developing the comprehensive analysis method reported herein, we thank The Ohio State University Comprehensive Cancer Center Comparative Pathology and Mouse Phenotyping Shared Resource (Director – Krista La Perle, DVM, PhD) for histology and immunohistochemistry services and the Pathology Imaging Core for algorithm development and analysis.

DISCLOSURES:

The authors have nothing to disclose.

REFERENCES:

1 Chambers, A. F., Groom, A. C., MacDonald, I. C. Dissemination and growth of cancer cells in metastatic sites. *Nature Reviews: Cancer.* **2** (8), 563-572 (2002).

2 Steeg, P. S. Targeting metastasis. *Nature Reviews: Cancer.* **16** (4), 201-218 (2016).

3 Gupta, G. P., Massague, J. Cancer metastasis: building a framework. *Cell.* **127** (4), 679-695 (2006).

4 Steeg, P. S. Tumor metastasis: mechanistic insights and clinical challenges. *Nature Medicine.* **12** (8), 895-904 (2006).

5 Chaffer, C. L., Weinberg, R. A. A perspective on cancer cell metastasis. *Science.* **331** (6024), 1559-1564 (2011).
6 Eckhardt, B. L., Francis, P. A., Parker, B. S., Anderson, R. L. Strategies for the discovery and development of therapies for metastatic breast cancer. *Nature Reviews Drug Discovery.* **11** (6), 479-497 (2012).
7 Gomez-Cuadrado, L., Tracey, N., Ma, R., Qian, B., Brunton, V. G. Mouse models of metastasis: progress and prospects. *Disease Models & Mechanisms.* **10** (9), 1061-1074 (2017).
8 Fantozzi, A., Christofori, G. Mouse models of breast cancer metastasis. *Breast Cancer Research.* **8** (4), 212 (2006).
9 Schoenenberger, C. A. et al. Targeted c-myc gene expression in mammary glands of transgenic mice induces mammary tumours with constitutive milk protein gene transcription. *EMBO Journal.* **7** (1), 169-175 (1988).
10 Nusse, R., Varmus, H. E. Many tumors induced by the mouse mammary tumor virus contain a provirus integrated in the same region of the host genome. *Cell.* **31** (1), 99-109 (1982).
11 Muller, W. J., Sinn, E., Pattengale, P. K., Wallace, R., Leder, P. Single-step induction of mammary adenocarcinoma in transgenic mice bearing the activated c-neu oncogene. *Cell.* **54** (1), 105-115 (1988).
12 Lin, E. Y. et al. Progression to malignancy in the polyoma middle T oncoprotein mouse breast cancer model provides a reliable model for human diseases. *American Journal of Pathology.* **163** (5), 2113-2126 (2003).
13 Green, J. E. et al. The C3(1)/SV40 T-antigen transgenic mouse model of mammary cancer: ductal epithelial cell targeting with multistage progression to carcinoma. *Oncogene.* **19** (8), 1020-1027 (2000).
14 Iorns, E. et al. A new mouse model for the study of human breast cancer metastasis. *PloS One.* **7** (10), e47995 (2012).
15 Kim, I. S., Baek, S. H. Mouse models for breast cancer metastasis. *Biochemical and Biophysical Research Communications.* **394** (3), 443-447 (2010).
16 Mariotto, A. B., Etzioni, R., Hurlbert, M., Penberthy, L., Mayer, M. Estimation of the Number of Women Living with Metastatic Breast Cancer in the United States. *Cancer Epidemiology, Biomarkers and Prevention.* **26** (6), 809-815 (2017).
17 Xiao, W. et al. Risk factors and survival outcomes in patients with breast cancer and lung metastasis: a population-based study. *Cancer Medicine.* **7** (3), 922-930 (2018).
18 Smid, M. et al. Subtypes of breast cancer show preferential site of relapse. *Cancer Research.* **68** (9), 3108-3114 (2008).
19 Kennecke, H. et al. Metastatic behavior of breast cancer subtypes. *Journal of Clinical Oncology.* **28** (20), 3271-3277 (2010).
20 Soni, A. et al. Breast cancer subtypes predispose the site of distant metastases. *American Journal of Clinical Pathology.* **143** (4), 471-478 (2015).
21 Leone, B. A. et al. Prognostic impact of metastatic pattern in stage IV breast cancer at initial diagnosis. *Breast Cancer Research and Treatment.* **161** (3), 537-548 (2017).
22 Pei, X. F. et al. Explant-cell culture of primary mammary tumors from MMTV-c-Myc transgenic mice. *In Vitro Cellular and Developmental Biology: Animal.* **40** (1-2), 14-21

(2004).
23 Mathsyaraja, H. et al. CSF1-ETS2-induced microRNA in myeloid cells promote metastatic tumor growth. *Oncogene.* **34** (28), 3651-3661 (2015).
24 Yang, S., Zhang, J. J., Huang, X. Y. Mouse models for tumor metastasis. *Methods in Molecular Biology.* **928** 221-228 (2012).
25 La Perle, K. M. D. Comparative Pathologists: Ultimate Control Freaks Seeking Validation! *Veterinary Pathology.* **56** (1), 19-23 (2019).
26 Blomberg, O. S., Spagnuolo, L., de Visser, K. E. Immune regulation of metastasis: mechanistic insights and therapeutic opportunities. *Disease Models & Mechanisms.* **11** (10) (2018).
27 Gonzalez, H., Hagerling, C., Werb, Z. Roles of the immune system in cancer: from tumor initiation to metastatic progression. *Genes and Development.* **32** (19-20), 1267-1284 (2018).
28 Borowsky, A. D. et al. Syngeneic mouse mammary carcinoma cell lines: two closely related cell lines with divergent metastatic behavior. *Clinical and Experimental Metastasis.* **22** (1), 47-59 (2005).
29 Yang, Y. et al. Immunocompetent mouse allograft models for development of therapies to target breast cancer metastasis. *Oncotarget.* **8** (19), 30621-30643 (2017).
30 Resch, M., Neels, T., Tichy, A., Palme, R., Rulicke, T. Impact assessment of tail-vein injection in mice using a modified anaesthesia induction chamber versus a common restrainer without anaesthesia. *Laboratory Animals.* **53** (2), 190-201 (2019).
31 Rashid, O. M. et al. Is tail vein injection a relevant breast cancer lung metastasis model? *Journal of Thoracic Disease.* **5** (4), 385-392 (2013).
32 Goodale, D., Phay, C., Postenka, C. O., Keeney, M., Allan, A. L. Characterization of tumor cell dissemination patterns in preclinical models of cancer metastasis using flow cytometry and laser scanning cytometry. *Cytometry Part A.* **75** (4), 344-355 (2009).
33 Goddard, E. T., Fischer, J., Schedin, P. A Portal Vein Injection Model to Study Liver Metastasis of Breast Cancer. *Journal of Visualized Experiments.* (118) (2016).
34 Wright, L. E. et al. Murine models of breast cancer bone metastasis. *BoneKEy Reports.* **5** 804 (2016).
35 Simmons, J. K. et al. Animal Models of Bone Metastasis. *Veterinary Pathology.* **52** (5), 827-841 (2015).
36 Liu, Z. et al. Improving orthotopic mouse models of patient-derived breast cancer brain metastases by a modified intracarotid injection method. *Scientific Reports.* **9** (1), 622 (2019).
37 Kodack, D. P., Askoxylakis, V., Ferraro, G. B., Fukumura, D., Jain, R. K. Emerging strategies for treating brain metastases from breast cancer. *Cancer Cell.* **27** (2), 163-175 (2015).
38 Brown, D. L. Practical Stereology Applications for the Pathologist. *Veterinary Pathology.* **54** (3), 358-368 (2017).
39 Aeffner, F. et al. Digital Microscopy, Image Analysis, and Virtual Slide Repository. *Institute for Laboratory Animal Research Journal.* **59** (1), 66-79 (2018).

Figure 1

Click here to access/download;Figure;JOVE Figure 1.eps

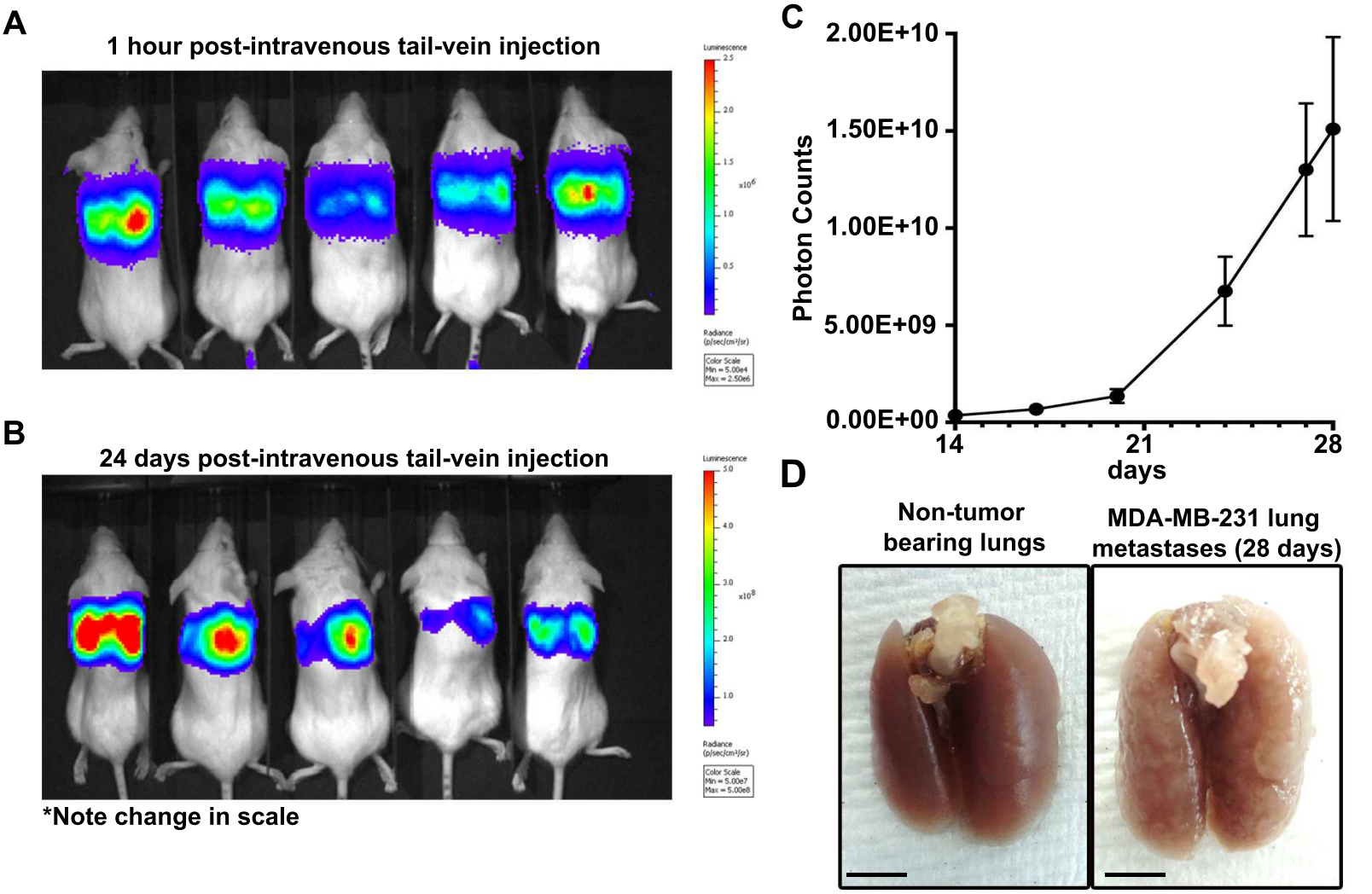

Figure 2

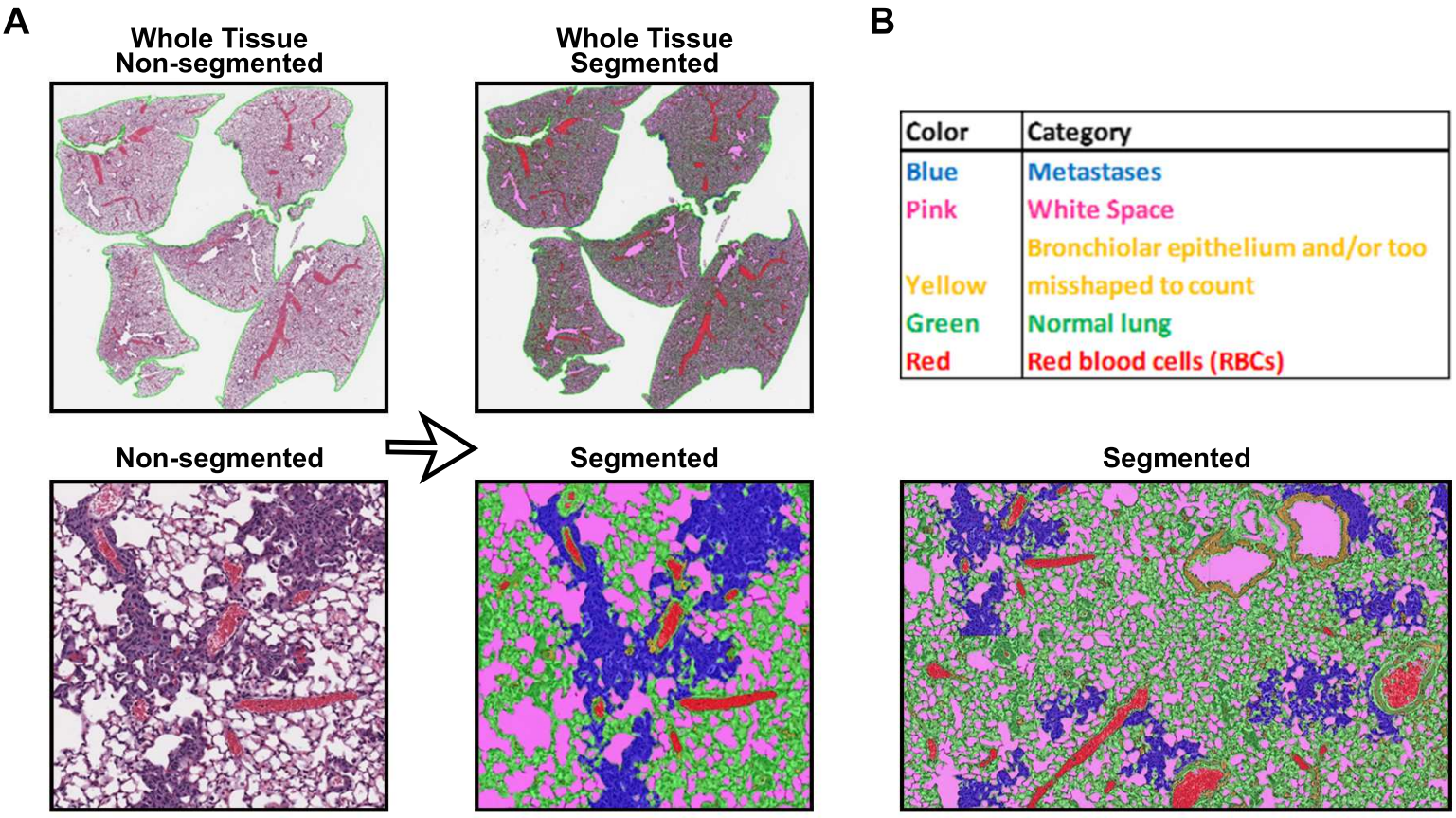

Figure 3

A

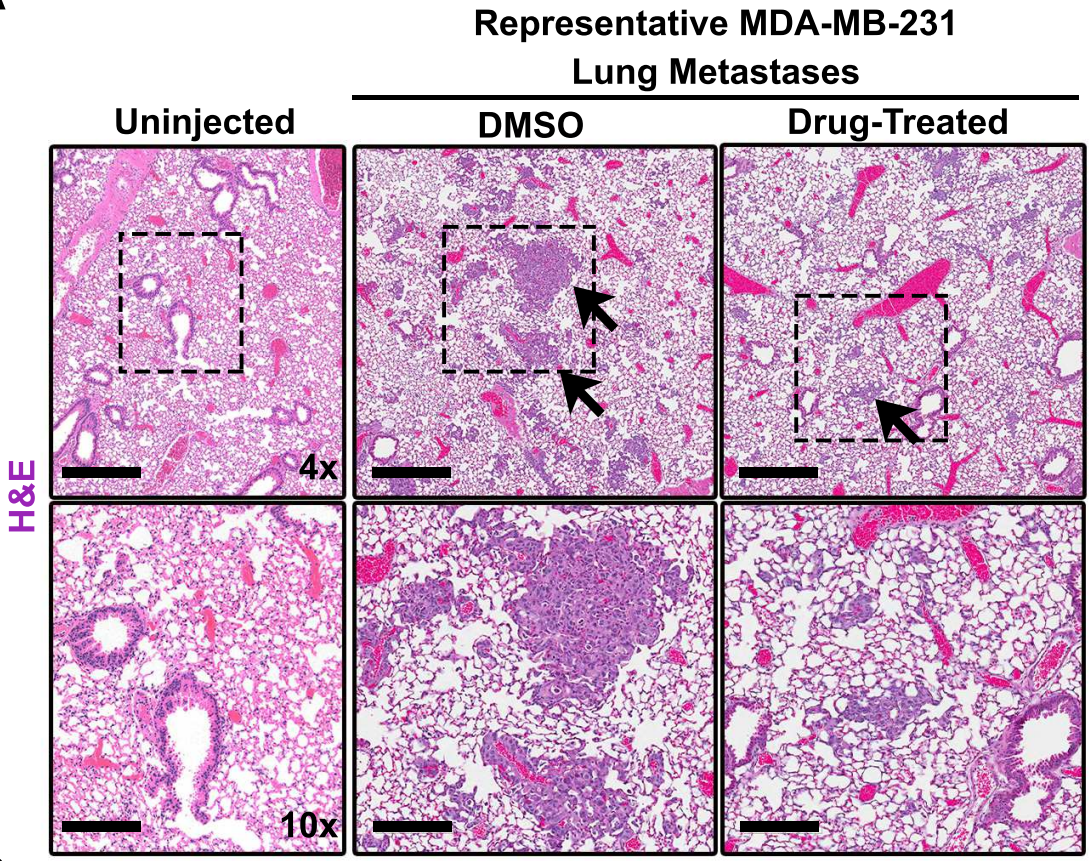

B

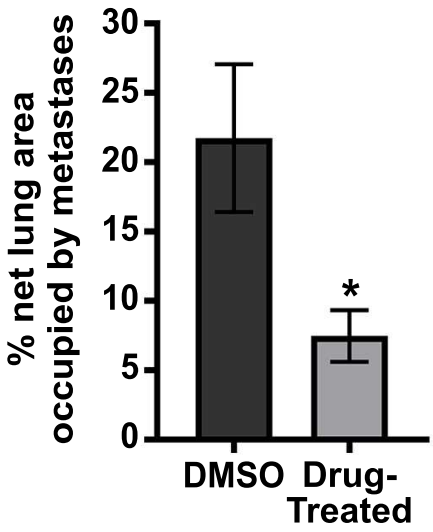

C

Parameter	DMSO (Ave ± SD)	Drug-Treated (Ave ± SD)	*P*-value
Lung metastasis count	503 (± 66.54)	400 (± 94.80)	0.389
% lung metastasis area	21.74 (± 5.32)	7.48 (± 1.86)	0.022
Total lung metastasis area (µm^2)	2.13E07 (± 4.98E06)	7.75E06 (± 2.38E06)	0.026
Net lung tissue area (µm^2)	9.65E07 (± 4.65E06)	9.37E07 (± 5.62E067)	0.707
Mean metastasis size (µm^2)	4.27E04 (± 1.18E04)	1.83E04 (± 1.59E03)	0.057
Median metastasis size (µm^2)	16955.54 (± 817.80)	14492.73 (± 804.33)	0.047

Table 1

Parameter	Description
Total Tissue Area (μm^2)	Area in square microns inclusive of all tumor metastases, normal lung and areas of red blood cells.
Metastasis Count	Total number of metastases within the lung tissue.
Metastasis Area Percentage (μm^2)	Total metastasis area divided by net tissue area x 100.
Total Tissue + White Space Area (μm^2)	Area in square microns inclusive of all tissue and white space.
Net Tissue Area (μm^2)	Tissue area in square microns (mets and normal lung) without white space and red blood cells.
Total Metastasis Area (μm^2)	Total metastasis area in square microns as segmented by the Decision Forest algorithim.
Mean metastasis Area (μm^2)	Mean (average) area in square microns of metastases within each image.
Median Metastasis Area (μm^2)	Median metastasis area in square microns. An equal number of metastases falls below this value and an equal number of metastases are greater than the median value.

Table 2

Click here to access/download;Table;JoVE_Table 2.xlsx

Slide	Metastasis Count	Metastasis Area Percentage (μm^2)	Total Tissue + White Space Area (μm^2)	Total White Space (μm^2)	Net Tissue Area (μm^2)	Total Metastasis Area (μm^2)	Red Blood Cells Area (μm^2)	Mean Metastasis Area (μm^2)	Median Metastasis Area (μm^2)
171 Lung Slide 1	435	8.90	185698000	83201800	92031400	8189250	10464800	18825.86	14748.73
171 Lung Slide 2	323	8.37	185698000	83201800	92054740	7708990	10441460	23866.84	14748.73
172 Lung Slide 1	151	2.73	181546000	89509904	81571296	2225220	10464800	14736.56	12486.37
172 Lung Slide 2	142	2.60	170708000	81735504	80558196	2093040	8414300	14739.72	12119.62
173 Lung Slide 1	634	11.60	234104992	102153000	115606692	13406800	16345300	21146.37	15472.22
173 Lung Slide 2	667	12.70	223180992	86778600	122374592	15542700	14027800	23302.40	16531.00
174 Lung Slide 1	40	0.55	192452992	80340896	87591096	485121	24521000	12128.03	10484.05
174 Lung Slide 2	34	0.51	183918000	71287904	91242796	464830	21387300	13671.47	11181.81
175 Lung Slide 1	780	23.93	179544992	44799200	126995782	30388600	7750010	38959.74	19307.76
175 Lung Slide 2	1001	12.58	169191536	43425608	120610754	15169100	5155174	15153.95	19703.08
188 Lung Slide 1	569	13.20	162290000	54210000	98486310	12997300	9593690	22842.36	14463.91
188 Lung Slide 2	271	5.15	157146000	54250800	91996500	4738100	10898700	17483.76	12657.83
189 Lung Slide 1	74	1.70	185292992	95700800	77779392	1318820	11812800	17821.89	14551.08
189 Lung Slide 2	74	1.76	182272992	95700800	74759392	1318820	11812800	17821.89	14551.08
816 Lung Slide 1	246	5.65	185876000	87568896	81916204	4631050	16390900	18825.41	14371.99
816 Lung Slide 2	565	6.05	183220000	76954304	90305396	5462670	15960300	9668.44	14244.82
876 Lung Slide 1	468	10.36	208308000	99300096	100947064	10454500	8060840	22338.68	16011.37
876 Lung Slide 2	528	11.74	199750896	81642568	110450391	12963400	7657937	24551.89	16699.13
877 Lung Slide 1	732	17.98	219340992	99918600	107869992	19397100	11552400	26498.77	18137.52
877 Lung Slide 2	605	14.64	207925504	88539712	108168329	15839700	11217463	26181.32	18014.64
878 Lung Slide 1	377	10.05	178534000	85610896	81931104	8232340	10992000	21836.45	16671.03
878 Lung Slide 2	376	9.88	170544000	75337904	86108406	8511710	9097690	22637.53	16754.38
879 Lung Slide 1	205	5.22	167556000	89999000	68123630	3553860	9433370	17335.90	13845.69
879 Lung Slide 2	213	4.64	167931008	80789400	78489588	3638720	8652020	17083.19	14058.12
881 Lung Slide 1	1122	38.81	218880000	79713504	130893816	50802300	8272680	45278.34	22044.99
881 Lung Slide 2	628	21.67	184200992	74502600	99122692	21475200	10575700	34196.18	19857.40
882 Lung Slide 1	678	24.05	194476992	83941904	98484788	23684500	12050300	34932.89	20748.06
882 Lung Slide 2	645	21.93	185537040	75790040	101412430	22241700	8334570	34483.26	20325.11
883 Lung Slide 1	429	10.79	179400992	84955696	84699866	9138800	9745430	21302.56	15080.23
883 Lung Slide 2	342	85.30	175220992	76210896	90472386	77170200	8537710	225643.86	17078.26
884 Lung Slide 1	359	6.42	206751008	87752600	103825008	6669710	15173400	18578.58	14333.41
884 Lung Slide 2	480	9.12	200990000	77052496	111060804	10125700	12876700	21095.21	15679.88
885 Lung Slide 1	332	7.79	191398000	92896304	84752596	6605490	13749100	19896.05	14500.11
885 Lung Slide 2	537	81.02	187475008	85938000	89378408	72411104	12158600	134843.77	15360.29
886 Lung Slide 1	305	7.93	158435008	80433296	76541662	6068720	1460050	19897.44	14500.11
886 Lung Slide 2	898	8.84	155460000	70808600	83457470	7380490	1193930	8218.81	14744.92

Table of Materials

Click here to access/download;Table of Materials;JoVE_Table_of_Materials.xlsx

Name of Material/Equipment	Company	Catalog Number	Comments/Description
alcohol prep pads	Fisher Scientific	22-363-750	for cleaning tail prior to injection
dissection scissors	Fisher Scientific	08-951-5	for mouse dissection and lung tissue inflation
DMEM with L-Glutamine, 4.5g/L Glucose and Sodium Pyruvate	Fisher Scientific	MT10013CV	cell culture media base for MDA-MB-231 and MVT1 cell lines
Dulbecco's Phosphate-Buffered Salt Solution 1x	Fisher Scientific	MT21030CV	used for resuspending tumor cells for injection
ethanol (70 % solution)	OSU		used to minimize mouse's fur during dissection; use caution - flammable
Evan's blue dye	Millipore Sigma	E2129	used at 1 % in sterile PBS for practice with tail-vein injection method; use caution - dangerous reagent
Fetal Bovine Serum	Millipore Sigma	F4135	cell culture media additive; used at 10% in DMEM
forceps	Fisher Scientific	10-270	for dissection and lung tissue inflation
FVB/NJ mice	The Jackson Laboratory	001800	syngeneic mouse strain for MVT1 cells
hemacytometer (Bright-Line)	Millipore Sigma	Z359629	for use in cell culture to obtain cell counts
insulin syringe (28 G)	Fisher Scientific	14-829-1B	for tail-vein injections (BD 329424)
MDA-MB-231 cells	ATCC		human breast cancer cell line
MVT1 cells			mouse mammary tumor cells
needles (26 G)	Fisher Scientific	14-826-15	used to inflate the mouse's lungs
neutral buffered formalin (10%)	Fisher Scientific	245685	used as a tissue fixative and to inflate lung tissue; use caution - dangerous reagent
NOD.Cg-Prkdcscid Il2rgtm1Wjl/SzJ (NSG) mice	The Jackson Laboratory	005557	maintained by OSUCCC Target Validation Shared Resource
Penicillin Streptomycin 100x	ThermoFisher	15140163	cell culture media additive
sterile gauze	Fisher Scientific	NC9379092	for applying pressue to mouse's tail if bleeding occurs
syringe (5 mL)	Fisher Scientific	14-955-458	used to inflate mouse lung tissue
tail-vein restrainer	Braintree Scientific, Inc.	TV-150 STD	used to restrain mouse for tail-vein injections
Trypan blue (0.4 %)	ThermoFisher	15250061	used in cell culture to assess viability
Trypsin-EDTA 0.25 %	ThermoFisher	25200-114	used in cell culture to detach tumor cells from plate

We thank the editorial team and reviewers for considering this body of work and for their critical assessment of our manuscript JoVE61270 "Pathological Analysis of Lung Metastasis Following Lateral Tail-Vein Injection of Tumor Cells". Several suggestions were made by both the editorial team and reviewers that we have been able to address. This includes the addition of data and text changes as well as our response to reviewers' comments (below). Changes to the text have been tracked throughout the revised version of the manuscript. Thanks to the reviewers, we believe this revision has improved the article, and it is now suitable for publication in *JoVE.*

Editorial comments:
General:
1. Please take this opportunity to thoroughly proofread the manuscript to ensure that there are no spelling or grammar issues.

All authors have carefully proofread the manuscript.

Protocol:
1. For each protocol step/substep, please ensure you answer the "how" question, i.e., how is the step performed? Alternatively, add references to published material specifying how to perform the protocol action. If revisions cause a step to have more than 2-3 actions and 4 sentences per step, please split into separate steps or substeps.

For the protocol, we have added details throughout to the steps/substeps that more directly answer "how" each step is to be performed.

Figures:
1. Please remove 'FIGURE 1' etc. from the figures themselves.

The FIGURE headings have been removed.

2. Figure 1C: What are the error bars?

Error bars represent the mean +/- SEM. This has been added to the figure legend on **page 7**.

3. Figure 2A: Please include scale bars.

Scale bars are not relevant as the images shown are snips of segmented and non-segmented images taken from slides originally scanned at 40x magnification. The Visiopharm platform is not a slide scanner itself and thus, when images are imported and segmented, they are not truly magnified. The figure legends on **page 7** have been updated to reflect this information, and **Figure 3** labels have been adjusted.

4. Figure 3: What statistical test was used to obtain p-values? What does '*' stand for?

'*' indicates statistical significance (i.e. *P*-value ≤ 0.05). For Figure 3B and 3C (table) all *P*-values were determined using a two-tailed Student's t-test following normality testing. This is now stated in the figure legend on **page 7**. Also, we have added a short paragraph to the results section that describes the statistical analysis that was done (**page 6**).

References:
1. Please do not abbreviate journal titles.

The references have been revised so as to not abbreviate journal titles.

Table of Materials:
1. Please ensure the Table of Materials has information on all materials and equipment used, especially those mentioned in the Protocol.

The Table of Materials includes information on all materials and equipment used.

Reviewers' comments:
Reviewer #1:
This is a valuable addition to a challenging area, well introduced and justified, and a particular strength is the cross-validation of tumour burden from the whole-animal bioluminescent studies to the histology. However, I do have some queries.

* The identification of cell densities in the H&E sections is asserted rather than shown. Ideally there would be further validation that these are cancer cells (not just, say, scars) using immunohistochemical markers or fresh sections with bioluminescence. But in the absence of this, a better illustration could be given showing more details of sections with and without tumour burden, so that the reader can be more clearly guided as to how the cancer/tumour areas are assessed. At present there is an assumption of pre-existing expertise in the reader, which I don't think is suitable for a manuscript that structured on being a detailed protocol/instruction.

To make this protocol more suitable for the novice reader/researcher, we have included a better illustration comparing the histology of metastatic tumor-bearing and non-tumor bearing lung sections in **Figure 3A**. Also, we have mentioned the use of immunohistochemical markers, such as E-cadherin, EpCAM, and cytokeratins as well as human-specific and tag-specific antibodies, on tissue sections as a means of further validation (**page 9**). Moreover, we have mentioned the use of TTF1 (transcription termination factor 1) as a maker for primary lung adenocarcinoma in cases where primary lung tumor development must be ruled out (**page 9**).

* Similarly, section 2.2.2 onward is vague. It would be nearly impossible for a reader to recapitulate the precise methods used here (and hence employ the protocol, or carry out a replication study). More detailed instructions are needed.

The Visiopharm platform provides many analysis algorithms or Apps to perform quantitative image analysis on digitized slides. There are a multitude of different solutions and algorithm approaches available. Once initial segmentation is performed, quality control of mark-ups may reveal deficiencies in the accurate identification of the structures to be measured with a particular algorithm. Fortunately, Visiopharm has the option of customizing algorithm, but as the software is robust, it requires hours of training for proficiency. The methodology presented herein is a description of the true methods for our particular study; however, particular studies may dictate the use of a different image analysis software platform or algorithm or may have to develop their own customized algorithms for their specific studies. With image analysis, “one size may not fit all”. Cellular morphology may differ between neoplastic cell lines. Familiarity and training are essential for all image analysis software platforms. Please see the discussion (**page 9**) for further information regarding choice of image analysis platform. More detailed instructions are now given in **section 2.2 (page 5)**.

* Again, showing images of the macroscopic lesions at necropsy would be valuable rather than left unshown.

Representative macroscopic MDA-MB-231 lung lesions at the time of necropsy are included next to normal, non-tumor bearing lung tissue in **Figure 1D.**

Reviewer #2:
Paper summary: The authors seek to provide a novel method of quantifying breast cancer (human MDA-MB-231; mouse MTV1) lung metastases after IV implantation.

Major Concerns:
None noted

Minor Concerns:
1. Suggested mouse strains used should be listed and for the mouse MVT1 model an immune-proficient mouse would be more physiologically relevant than an athymic or other immune deficient model, as most steps of metastasis are highly dependent on the immune system.

This is an excellent point. We have now provided suggestions on mouse strains and commented on the advantage of an immune-proficient (FVB/N strain) mouse model using the MVT1 cells. The limitation of athymic or immune deficient models is also included in the discussion (**pages 2 and 8**).

2. Some discussion (in addition to the literature references cited in the manuscript) of the choice of cell implantation number should be given as the cell numbers (1 million MDA-MB-231; 3 million MVT1) are large and overwhelming to the lungs and as such may not represent typical metastatic colonization, immune reaction, death, etc.

We appreciate the reviewer's attention to this matter. To address this, we have included discussion on the choice of cell number and acknowledged the drawback to intravenous injection of such a large number of cells. This is now included as part of the critical steps on **pages 8.**

3. In keeping with the comment above, using a narrow-gauge needle (28G) may be less painful to the animal and easier to inject into the tail vein, but pushing cells through the needle can lead to large amounts of damaged/dead cells, complicating the interpretation of the results

We agree with the reviewer that the narrow-gauge needle may contribute to cell death and therefore, misinterpretation of the results. We have included a statement on **page 9** to acknowledge this limitation and possible confounding factor.

4. The Visiopharm Image Analysis software is absolutely critical to the innovation and ultimate successful outcome of this work and the approximate cost associated with this software and whether any free alternatives are available should be made clear in the discussion section

Considerations for choice of image analysis software, including cost, availability, and experience level, etc. have been added to the discussion section on **page 9**. Alternative imaging platforms are mentioned as well.

5. In the future directions section, more physiologically relevant orthotopic mammary fat pad implantation methods should be mentioned, as the direct IV injection (as the authors note) bypasses several steps of metastasis and has the drawbacks noted in second and third points above.

We apologize for overlooking this important point and have included within the discussion a statement on more physiologically relevant models for which the method of lung tumor burden analysis would still be applicable (**pages 9-10**). The drawbacks to direct intravenous injection of cells has been elaborated on as well (**page 9**).